MIMO Spatial Multiplexing with an Array of Tilted Leaky-Wave Antennas for Terahertz Communications

Albert Diez Comas*, Duschia Bodet*, Zhaoji Fang†, Hichem Guerboukha‡, Daniel M. Mittleman†, Josep M. Jornet*

*Northeastern University, Boston, MA, USA E-mail: {diezcomas.a, bodet.d, jmjornet}@northeastern.edu
†Brown University, Providence, RI, USA E-mail: {zhaoji_fang, daniel_mittleman}@brown.edu
‡University of Missouri-Kansas City, MO, USA E-mail: hichem.guerboukha@umkc.edu

2023 IEEE Future Networks World Forum (FNWF) | 979-8-3503-2458-7/23/$31.00 ©2023 IEEE | DOI: 10.1109/FNWF58287.2023.10520437

***Abstract*—This study explores the potential application of leaky-wave antennas (LWA) in Terahertz (THz) Multiple-Input Multiple-Output (MIMO) systems to achieve spatial multiplexing and enhance data rates. The THz band's unique features, offering wide bandwidths and Tera-bit-per-second (Tbps) links, make it an attractive solution for meeting the ever-growing data traffic demands in 6G and Beyond wireless systems. However, the transition to the THz band poses some challenges, including high path loss due to small wavelengths. To address these challenges, this paper proposes employing LWAs that not only offer high directivity but also enable dynamic beam steering without complex feeding systems. Spatial multiplexing is achieved by tilting the elements of a LWA array, allowing to transmit independent data streams with minimal interference, thereby facilitating higher data rates. This approach overcomes previous bandwidth limitations of LWA arrays and proves effective even in highly dense scenarios.**

***Index Terms*—Terahertz (THz), MIMO, leaky-wave antenna (LWA), array, spatial multiplexing, tilted LWA array**

I. Introduction

Terahertz (THz) band communications are envisioned as one of the key enabling technologies to satisfy the exponential growth of data traffic volume, as well as the increasing demand for higher data rates and improved coverage in 6G and Beyond wireless systems [1], [2]. The THz band, spanning from 0.1 to 10 THz, offers bandwidths on the orders of tens of Gigahertz (GHz) interspersed with atmospheric absorption peaks, which have the potential to enable Tera-bit-per-second (Tbps) links [3]. However, despite the opportunities THz communications bring, it also comes with its own challenges.

One major obstacle in transitioning to the THz band is the high path loss. The small wavelengths at these frequencies result in antennas with very small effective areas, leading to significant spreading losses. Nonetheless, the small antenna sizes create opportunities for implementing arrays with a large number of antennas, which has led to the proposal of Multiple Input Multiple Output (MIMO) systems for THz systems [4]–[7]. MIMO systems aim to combat the high path losses and improve the achievable data rates by employing multiple antennas to transmit either single or multiple data streams.

This work was funded by NSF grants NSF-2211616 and NSF-1954780 and the Air Force Office of Scientific Research FA9550-22–1-0412.

In the case of sending a single stream, beamforming can be employed by adjusting the phases at each antenna to manipulate the radiation pattern of the antenna array. This constructive interference enhances the signal-to-noise ratio (SNR) of the channel, thereby mitigating the high path loss. On the other hand, multiple antennas can be utilized to send multiple data streams through spatial multiplexing. Although spatial multiplexing is typically accomplished by exploiting phase variations in multipath propagation at lower frequencies, it is not as prevalent at THz frequencies due to the predominance of line-of-sight (LoS) propagation [8], [9]. Hence, alternative methods must be considered to obtain spatial multiplexing.

A proposed approach for achieving spatial multiplexing in LoS scenarios involves leveraging optimal antenna allocation via reconfigurable array architectures [10], [11]. Reconfigurable arrays use the phase differences generated by a spherical wavefront across distinct antenna elements to separate the multiplexed signals. This phenomenon is particularly prevalent at THz frequencies, as they often operate in the near-field region. Nevertheless, this solution presents practical challenges, such as the need for consistent optimal allocation as the receiver moves and the dependence of the configuration on frequency, limiting its viability in wideband scenarios.

Other alternatives include using directional antenna elements to enhance data rates in THz systems [12]. Directional antennas not only increase received power but also enable the transmission of multiple data streams if each transmitting antenna points to a different receiving antenna, ensuring only one LoS component per antenna pair. Similarly, a beamforming array may also act as a directional antenna with beam steering capabilities. An architecture comprising an array of subarrays can be employed, enabling the transmission of independent data streams over each subarray [5], [13].

Lastly, ongoing exploration is being conducted to investigate the potential of multiplexing diverse co-propagating beams via orbital angular momentum (OAM), with the aim of increasing the channel capacity [14], [15]. Within this context, the concept revolves around the ability to multiplex numerous data streams distinguished by distinct OAM mode values, which due to their orthogonal characteristics, can be efficiently demultiplexed upon reception without much interference.

In this paper, we explore the use of leaky-wave antennas (LWA) [16], [17] as directive antenna elements for THz MIMO systems. LWAs are radiating structures whose radiation direction depends on the excitation frequency, allowing for dynamic beam steering without requiring complex feeding systems like phase shifters. Additionally, their elongated nature often results in high directivity, with a beam narrow in the scanning angle and wide in the cross-plane. However, the main drawback of LWAs is their limited usable bandwidth in a specific direction.

The utilization of arrays of LWAs has been proposed in several papers to achieve three-dimensional beamforming using a linear array setup, unlike the planar arrays required for conventional (semi-)omnidirectional antennas [18]–[21]. By adding phase shifters at the input of each LWA, a fixed-frequency beam can be scanned in the cross-plane in addition to the frequency scanning along the scanning plane. Furthermore, through the arrangement of a linear LWA array, it becomes feasible to narrow the radiated beam in the cross-plane, leading to a high spatial resolution in both dimensions.

In this study, we investigate the potential effectiveness of employing the frequency-scanning nature of LWAs in THz communications. Specifically, we propose tilting the antenna elements of the LWA array to obtain spatial multiplexing instead of beamforming. The concept behind this approach is that, by tilting the elements of the array, each LWA can transmit independent data streams with minimal interference, thereby facilitating higher data rates. Moreover, this strategy effectively overcomes the main bandwidth limitation that previously hindered the use of LWAs in communications, as different LWA elements will utilize different frequencies for a particular transmission direction. Additionally, we introduce a stair-case LWA array design intended for multi-user scenarios, enabling users communicating with the LWA array to achieve exceptionally high data rates.

In Sec. II, we present a comprehensive description of the THz MIMO channel, accompanied by the formulation of the necessary capacity equations. Moving forward, in Sec. III, we delve into an in-depth exposition of various LWA array configurations. The performance evaluation of these arrays is conducted in Sec. IV with numerical analysis. Lastly, the conclusive findings of our study are provided in Sec. V.

II. THz LoS MIMO Communication

A. MIMO Channel Modeling

MIMO systems typically rely on multipath propagation to transmit independent data streams through spatial multiplexing. However, in the THz band, due to the fact that the roughness of most surfaces is comparable to the wavelength, scattering and reflection losses become very high. Consequently, multipath propagation becomes weak, and the channel response is primarily dominated by LoS propagation [8], [9].

Moreover, when studying the performance of LWAs in a MIMO system, it is important to include the radiation pattern of the antenna elements into the channel response. Additionally, when considering a wide bandwidth, the frequency dependence of the spreading losses and the radiation pattern of LWAs must be considered. From these considerations, the channel response between transmitter m and receiver n can be defined as

$$h_{n,m} = \alpha(d_{n,m}, \lambda)\beta(\theta_{n,m}, \phi_{n,m}, \lambda)e^{-j2\pi/\lambda d_{n,m}}, \quad (1)$$

where $\alpha(d_{n,m}, \lambda) = \lambda/4\pi d_{n,m}$ is the propagation loss characterized by the spreading loss, which depends on the wavelength λ and the relative distance between the antenna pairs $d_{n,m}$. Meanwhile, $\beta(\theta_{n,m}, \phi_{n,m}, \lambda)$ is the radiation pattern of the antenna element, which depends on the wavelength and the relative elevation angle $\theta_{n,m}$ and azimuth angle $\phi_{n,m}$ between the antenna elements. The reader might have observed the absence of the molecular absorption response in (1), which many papers use to characterize the channel response at THz frequencies [7], [22]. The omission is justified as it is considered negligible at the operating frequency and the distances investigated in this paper, which will be further explained in Sec. IV.

The LoS MIMO channel matrix can then be represented as

$$\mathbf{H} = \begin{bmatrix} h_{1,1} & h_{1,2} & \cdots & h_{1,N_{tx}-1} & h_{1,N_{tx}} \\ h_{2,1} & h_{2,2} & \cdots & h_{2,N_{tx}-1} & h_{2,N_{tx}} \\ \cdot & \cdot & & \cdot & \cdot \\ \cdot & \cdot & & \cdot & \cdot \\ \cdot & \cdot & & \cdot & \cdot \\ h_{N_{rx}-1,1} & h_{N_{rx}-1,2} & \cdots & h_{N_{rx}-1,N_{tx}-1} & h_{N_{rx}-1,N_{tx}} \\ h_{N_{rx},1} & h_{N_{rx},2} & \cdots & h_{N_{rx},N_{tx}-1} & h_{N_{rx},N_{tx}} \end{bmatrix}, \quad (2)$$

which groups the channel responses between each antenna pair and has a size of $N_{rx} \times N_{tx}$, with N_{rx} and N_{tx} being the number of receiving and transmitting antennas, respectively.

B. Capacity in a Point-to-Point MIMO Channel

The performance of a MIMO system is characterized by the Shannon capacity, which represents the maximum achievable data rate. Because of the frequency-scanning behavior of LWAs, we will consider the case where the transmitter has knowledge of the channel, allowing the use of the proper frequency for the transmission in a specific direction. In this case, the capacity over a bandwidth B, assuming an invariable channel, can be obtained using the water-filling algorithm [23], and it can be measured as

$$C = B \sum_{i=1}^{n_{min}} \log\left(1 + \frac{P_i \lambda_i^2}{N_0 B}\right) \text{(bits/s)}, \quad (3)$$

where n_{min} is the rank of $\mathbf{H}$, or equivalently the number of non-zero singular values of $\mathbf{H}$. $P_1, \ldots, P_{n_{min}}$ are the water-filling power allocations, $\lambda_1, \ldots, \lambda_{n_{min}}$ are the singular values of the channel matrix $\mathbf{H}$, and $N_0 = k_B T$ is the noise spectral density where k_B is the Boltzmann's constant and T is the temperature. Figure 1a shows a representation of the water-filling algorithm when considering n_{min} spatial sub-channels over an invariable channel. In the figure, the value μ is chosen to satisfy the total power constraint $\sum_i P_i = P$.

However, in order to examine the frequency dependency of the path loss and the radiation pattern of the LWA, the channel response variance over a wide bandwidth must be accounted. Hence, water-filling should be performed not only over the different transmitting antennas but also over the

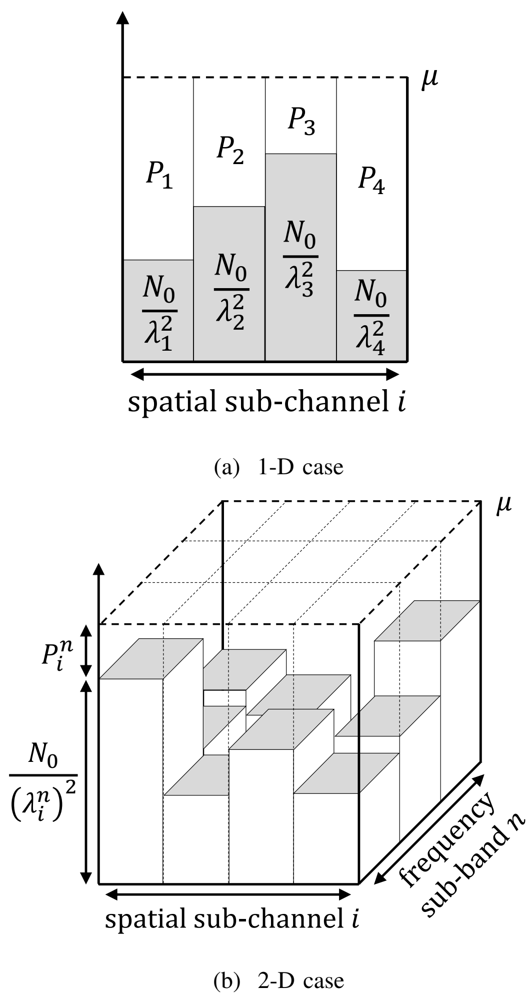

Fig. 1. Principle of the water-filling algorithm.

bandwidth of interest. The representation of the algorithm over the two dimensions is shown in Fig. 1b. The bandwidth B is divided into equal sub-bands Δf, ensuring that the channel can be considered invariant over each sub-band, and then water-filling can be performed over both variables. The transmitter optimally allocates power over different antennas and sub-bands, and the capacity over the entire bandwidth can be calculated as

$$C = \Delta f \sum_{n=1}^{N_{bands}} \sum_{i=1}^{n_{min}} \log \left(1 + \frac{P_i^n {\lambda_i^n}^2}{N_0 \Delta f} \right) \text{(bits/s)}, \tag{4}$$

where N_{bands} is the number of sub-bands inside the total bandwidth B. P_i^n and λ_i^n are the water-filling power allocations and the singular values of the channel matrix, respectively, for a particular spatial sub-channel i and sub-band n. The power is distributed over the antennas and frequencies such that it still satisfies the total power constraint $\sum_n \sum_i P_i^n = P$.

C. Capacity in a Multi-User Channel

For scenarios where multiple users need to share the same channel, the principles of information theory can be extended from a one-to-one setup to a multi-user setup. These systems usually consist of a single base station that simultaneously communicates with multiple users. By equipping the base station with multiple antennas, multi-user MIMO systems can be employed, allowing for spatial multiplexing and increased diversity for each user [23], [24]. This enables the transmission and reception of data from multiple users at high rates.

MIMO techniques have been extensively studied for single-user scenarios, and it is well-known that the capacity of a MIMO system can increase linearly with $min(N_{tx}, N_{rx})$. However, determining the capacity in a multi-user scenario is more complex. Nevertheless, recent findings suggest that a similar capacity scaling is observed when a base station with N_{tx} antennas communicates with N_{rx} users [25], which justifies the use of multiple antennas in base stations for multi-user scenarios.

The multi-user MIMO channel can be defined as in the single-user case, using a channel matrix as described in (2). In this case, the N_{rx} receivers are distributed among several users, where each user may have one or multiple antennas. Consequently, the N_{rx} receive antennas are distributed among N_{users}, with $N_{users} \leq N_{rx}$.

In a point-to-point channel, independent data streams can be created by processing the signals between all the transmitters and receivers. However, in a multi-user channel, coordination between users is usually absent, and the processing is limited to the signals received by each user individually. This inherent asymmetry in the channel gives rise to differences between the uplink and downlink channels. In the uplink, a group of users attempts to communicate with the same base station, necessitating the separation of signals from different users at the base station. In the downlink, the base station aims to communicate with multiple users, requiring the transmission of signals in a manner that allows each user to separate their own signal from those intended for other users.

The presence of multiple users introduces a new variable in capacity measurement, allowing for different power allocations to different users in the network. This leads to a capacity region, which defines the achievable information rates for users based on the power allocated to each one, given a constraint on the total transmitted power. The maximum capacity of the system is determined by a point that maximizes the sum of the information rates for all users, often referred to as the sum capacity. However, due to the various possibilities for power allocation among users, determining the capacity of a multi-user channel can be quite complex and often requires complex data processing and user cooperation, which may be challenging to achieve in certain applications. Instead, in this paper we will focus on measuring the sum capacity when the transmitter allocates its resources to the user with the strongest channel response at a given frequency. Although it may not be the maximum achievable capacity, it generally provides a near-optimal result and is straightforward to measure.

Let us consider only the downlink communication of a multi-user channel and assume that each user has one antenna, such that $N_{rx} = N_{users}$. The proposed method of resource allocation to the stronger user operates as follows: The base station possesses knowledge of the channel between each transmit and receive antenna pair for each sub-band

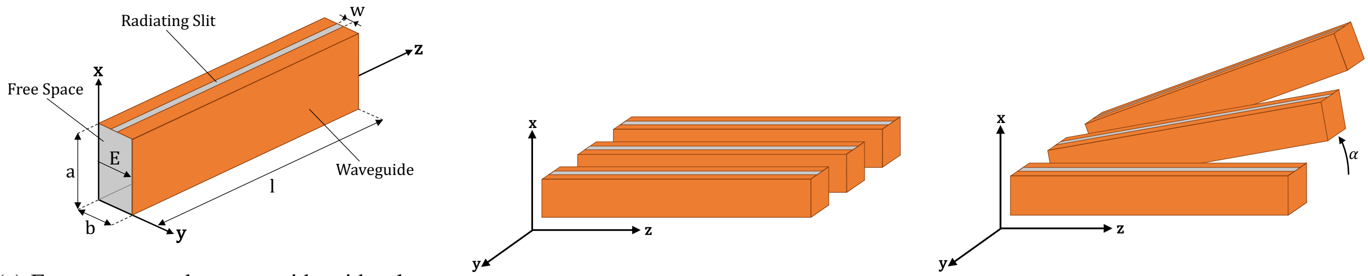

(a) Empty rectangular waveguide with a longitudinal slit in the narrow wall

(b) Uniform LWA array

(c) Tilted LWA array

Fig. 2. Representation of the LWA under study and the different LWA array architectures.

(represented by the channel matrix **H**). Then, each transmit antenna chooses the user with the strongest channel response at each sub-band (i.e., the best $h_{n,m}$ from every column of **H**). Finally, the water-filling algorithm is applied across the transmit antennas and frequencies. Consequently, the total power in the base station is optimally allocated between the transmit antennas, each transmitting to the users with the best channels. The data rates of the users are then determined based on the signal-to-interference-plus-noise-ratio (SINR), where the power allocated by each transmit antenna to the intended user constitutes the signal of interest, and the received signal intended for other users is treated as interference. Thus, the resulting data rates for a user k can be calculated as

$$R_k = \Delta f \sum_{n=1}^{N_{bands}} \log\left(1 + \frac{\sum_{i=1}^{N_{tx}} P_{k,i}^n |h_{k,i}^n|^2}{N_0 \Delta f + \sum_{i=1}^{N_{tx}} \sum_{\substack{j=1 \\ j\neq k}}^{N_{rx}} P_{j,i}^n |h_{k,i}^n|^2}\right), \quad (5)$$

where $|\cdot|$ represents the absolute value operator. $P_{j,i}^n$ is the power allocated in the transmit antenna i to send data to the user j for the sub-band n, and $h_{j,i}^n$ is the channel response between transmitter i to receiver j for the sub-band n. The sum capacity can then be defined as the sum of the rates for all users, i.e. $C = \sum_{k=1}^{N_{users}} R_k$.

III. Leaky-Wave Antenna Arrays

Having established the appropriate channel modeling for THz MIMO communications, considering the radiation pattern of the antenna elements and the frequency variance across a wide bandwidth, we can now introduce different array architectures that take advantage of the frequency-scanning behavior of LWAs.

In the remaining sections of the paper, the LWA design being investigated is the rectangular waveguide LWA [26]. This type of LWA consists of an empty rectangular waveguide with a longitudinal slit in the narrow wall that operates in its fundamental mode, as can be seen in Fig. 2a. The rectangular waveguide LWA is a uniform type, hence it transmits solely in the forward direction. This design has been chosen for its simplicity and its ability to provide a general understanding of the proposed system. Nevertheless, the insights presented in this paper can be extended to other LWA designs as well.

Traditional LWA arrays are typically distributed uniformly in a linear array. However, in this paper, we propose a different approach of array architecture where each LWA is slightly tilted compared to the neighboring one. In this way, the array is able to reuse the frequencies to reach the different receivers, thereby enhancing spectral efficiency. The following sections provide a more detailed description of these architectures.

A. Uniform Linear Array of Leaky-Wave Antennas

The conventional method of arranging an array of LWAs involves uniformly distributing them side by side in an array, as can be seen in Fig. 2b. This arrangement enables three-dimensional beamforming using a linear array of LWAs, where phase-shifters are placed on each element. By setting a linear consecutive phase between each element, azimuth plane (X-Y plane) scanning is performed, while elevation plane (Z-X plane) scanning is achieved through frequency-scanning techniques. This approach of beamforming with LWAs is cost-effective, simple, and efficient compared to traditional phased-arrays using omni-directional antennas, as it requires less phase shifters. Due to the high directivity of LWAs, fewer elements are needed to achieve a certain gain compared to traditional phased-arrays. However, the frequency dependence with the scanning angle limits the usable bandwidth in a specific direction, and fixed-frequency beam-steering is not possible unless reconfigurable LWAs are employed [27]–[29].

The frequency-scanning behavior of LWAs can be utilized to transmit different data streams toward distinct directions. Frequency-division multiplexing (FDM) [30] can be employed by dividing the total bandwidth into non-overlapping bands, with each band carrying a separate signal transmitted toward a different direction. However, while the signal can be divided in space, it cannot strictly be considered spatial multiplexing as different frequencies need to be used. In other words, the spectral efficiency is lower than it would be for true spatial multiplexing where the system is simultaneously multiplexing users using space and frequency.

B. Tilted Array of Leaky-Wave Antennas

A LWA can be viewed as a radiating element that separates the frequency spectrum of the input signal into different angles, directing a narrowband signal with a specific center frequency toward a particular direction. Now, let us consider

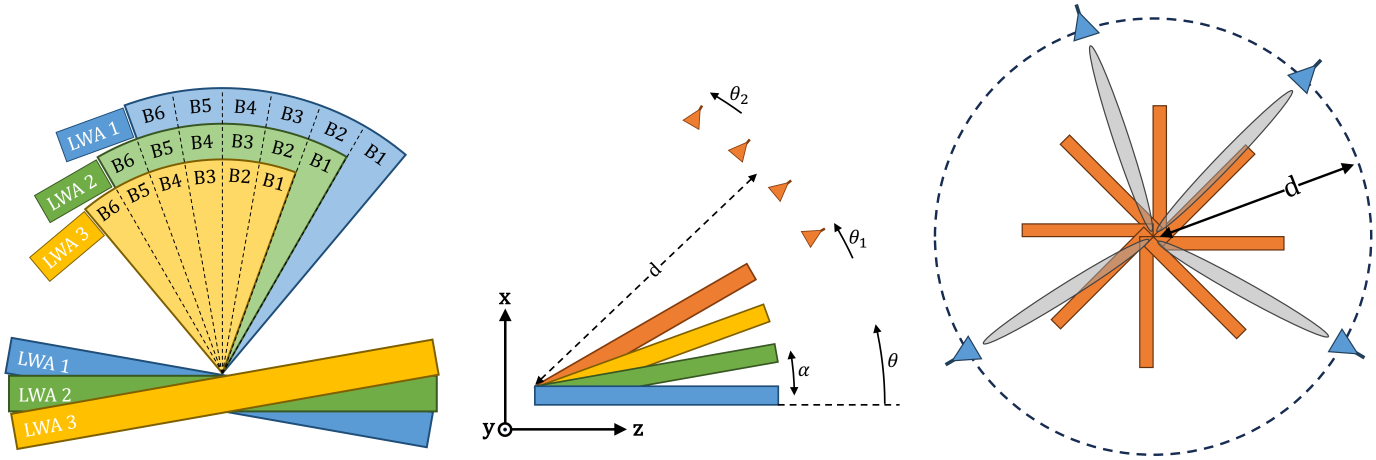

(a) Spatial multiplexing characteristics using a tilted LWA array

(b) Tilted LWA array in a point-to-point MIMO system

(c) Stair-case LWA array in a multi-user MIMO system

Fig. 3. Representation of the proposed LWA arrays in MIMO systems.

an array of LWA. If all LWA are uniformly positioned, they will transmit towards the same direction when using the same carrier frequency for different signals. This limits non-interfering transmission to beamforming, as described in the previous subsection. In beamforming, the same signal is sent over all LWAs, which increases received power but does not improve spectral efficiency.

The proposed approach in this paper is to apply a consecutive angle tilt to each array element, causing each LWA to be slightly tilted over the scanning range. Figure 2c shows the array architecture, which we will refer to as tilted LWA array. Applying a tilt to the array elements enables them to transmit toward different directions at a given carrier frequency. To avoid interference, the tilt between each antenna must exceed the beamwidth of the radiated beam. Using this tilted array architecture with LWA offers several advantages, as it allows for transmitting different data streams over different frequencies and antennas, leveraging frequency multiplexing and spatial multiplexing simultaneously.

Figure $3a$ illustrates how spatial multiplexing is achieved with the array design. The plot showcases the tilted LWA array geometry, where spatial multiplexing is achieved through the frequency-dependent behavior of the LWAs. The operational bandwidth of the LWA is divided into multiple sub-bands (B1, B2, ...), within which the radiation pattern of the LWA remains relatively constant. Within a particular sub-band, the LWAs radiate the beam mainly towards the represented directions. Consequently, due to the different tilts of the LWAs in the array, each LWA independently transmits signals within a specific sub-band towards different directions, as long as the tilt is greater than the beamwidth for the given sub-band. This design offers the advantage of being able to simultaneously transmit as many independent signals as number of LWAs, while also allowing for the utilization of multiple sub-bands to transmit towards a particular direction, which improves the bandwidth usage. This array configuration precludes beamforming, as the transmit antennas cannot send the same signal at a specific frequency to the same direction. Nonetheless, the LWA itself is a directive antenna, benefiting from the high gain typical of phased-arrays.

Now let us consider the system model depicted in Fig. $3b$. The scenario comprises multiple transmitting LWA and several receiving arbitrary antenna elements. We assume that the receiving antennas are perfectly isotropic and capable of operating over the same entire bandwidth as the LWA. The transmitting LWAs are positioned along the y-axis with a consecutive tilting angle α. The receiving antennas are distributed uniformly in an arc geometry between elevation angles θ_1 and θ_2, located at a distance d from the transmit array and residing ideally within the scanning range of all the transmitting LWAs. Assuming that the transmitter possesses perfect channel knowledge, the power can be allocated among the antennas using the water-filling algorithm. Each antenna transmits at the corresponding frequencies to direct the signal towards the intended receivers.

C. Stair-case Array of Leaky-Wave Antennas

The concepts derived from the tilted LWA array can be extended to an array of LWAs covering the entire 360° range. By placing the LWAs on top of each other, each with the radiating slit positioned to the side, it becomes possible to engineer a transmitting array capable of scanning the beam to different angular directions. This array of LWAs enables the transmission of multiple data streams in different directions, either by utilizing distinct frequency bands or by transmitting through separate antennas. We refer to this architecture, depicted in Fig. $3c$, as a stair-case LWA array due to its resemblance to a spiral stair-case in terms of geometry. The narrow beamwidth of LWAs in the scanning angle allows for effective separation of different data streams in space with high angular resolution. This characteristic proves advantageous in achieving high capacities through multiple independent channels created by the frequency-dependent radiation pattern of LWAs. The stair-case array architecture shows promise for deployment as base stations, particularly in densely populated scenarios. If the base station possesses knowledge of the receiver positions or,

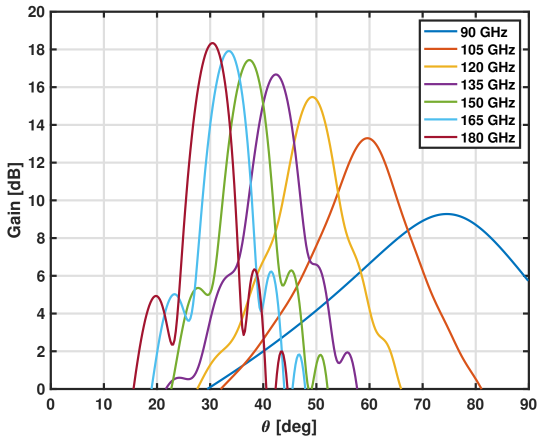

(a) Scanning plane

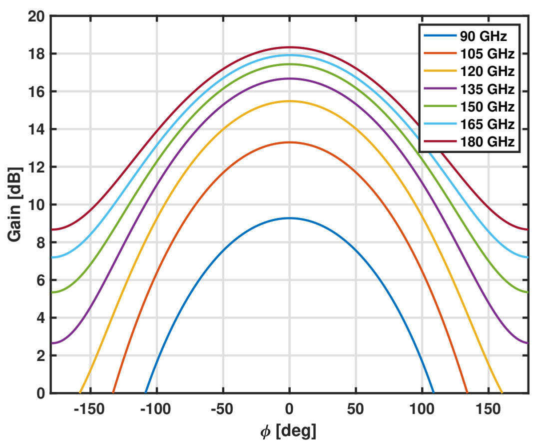

(b) Cross-section plane

Fig. 4. Simulated radiation pattern of the rectangular waveguide LWA.

ideally, their channel responses, the water-filling algorithm can be applied for an optimum power allocation between antennas and frequencies, resulting in significantly high capacities.

Similarities can be observed between the stair-case array of LWAs architecture and sectorized antenna arrays. Both involve antenna elements pointing toward different angular directions. Sectorized antennas are directional antennas with sector-shaped radiation patterns that offer high gain across a range of angles. Sectorization is commonly used in cellular system base stations to reduce interference. The advantage of the stair-case LWA array lies in its beam-steering capabilities. Due to the frequency-scanning behavior of LWAs, it is possible to have a narrow beamwidth while covering a wide range. In contrast, sectorized antennas can only cover the range allowed by their fixed beamwidth. This brings two distinct approaches. Firstly, the narrow beamwidth of LWAs can provide high gain while covering a wide area. Secondly, the narrow beamwidth allows for an array of highly packed tilted antenna elements, each capable of transmitting independent data streams, offering a new approach to achieving high capacities through spatial multiplexing in MIMO systems.

IV. Numerical Results

A. Capacity of Tilted LWA Array

A numerical analysis is performed on the architecture shown in Fig. $3b$, which represents a $4{\times}4$ MIMO system, in order to evaluate the performance of the tilted LWA array described in Sec. III-B. The dimensions of the waveguide, depicted in Fig. 2a, are a width a of 1.651 mm and a height b of 0.825 mm. Hence, the fundamental mode TE_{10} operates between frequencies of 90.791 and 181.583 GHz. The width of the slit w is 165 μm, and the length of the waveguide is chosen to be 30 mm, ensuring that more than 90% of the radiation power is radiated before reaching the end of the waveguide.

To obtain the radiation pattern of the LWA within this frequency range, an electromagnetic simulation using full wave finite-element-method (FEM) with COMSOL Multiphysics is performed. Figures $4a$ and $4b$ illustrate the simulated radiation patterns for various frequencies, represented on the scanning plane and the cross-section plane, respectively. In the first plot, it can be seen how the antenna steers with frequency, starting from nearly broadside ($\theta = 90°$) at the cutoff frequency and gradually reaching the end-fire ($\theta = 0°$). The characteristic gain increase, typical in LWAs, is observed as the radiation approaches the end-fire direction, with a maximum value that goes from around 9 dB to 18 dB. The second plot shows the radiation pattern within the cross-section plane. It can be seen that, while the radiated beam is narrow in the scanning plane, it is considerably broader in the cross-section plane.

The transmitting LWAs are arranged in a tilted array configuration, while the receivers are uniformly positioned at the angles θ from 30° to 60°, ensuring that they all fall within the scanning range of the LWAs. The capacity is evaluated from (4) for various transmission distances ranging from 0.1 to 10 m and different tilting angles ranging from 0° to 10°. The total available transmit power is 1 W, the receiver temperature is 300 K for measuring the noise spectral density, and the total bandwidth is divided into sub-bands of 1 GHz.

The obtained capacities are depicted in Fig. $5a$ and $5b$, as a function of the transmission distance and the tilting angle, respectively. The results demonstrate that higher capacities are achieved as the tilt between the array elements increases, leading to enhanced spatial multiplexing capabilities. Nevertheless, there comes a threshold beyond which the scanning range of some LWAs exceeds the positions of the receivers, thereby limiting further performance improvements.

B. Capacity of Stair-Case LWA Array

We propose utilizing the stair-case LWA array, as described in Sec. III-C, as a base station for multi-user communication systems. To evaluate its performance, we conducted a numerical simulation on the architecture shown in Fig. 3c of a multi-user scenario and we show a comparison with a sectorized antenna array. The gain of the sector antenna is calculated through its relation to the beam solid angle $D = \frac{4\pi}{\Delta\theta\Delta\phi}$, where $\Delta\theta$ and $\Delta\phi$ denote the beamwidth in radians in the elevation angle and the azimuth angle, respectively. These angles are presumed to be 45° and 90°, respectively, to have similar values than the simulated LWA. This yields a calculated gain

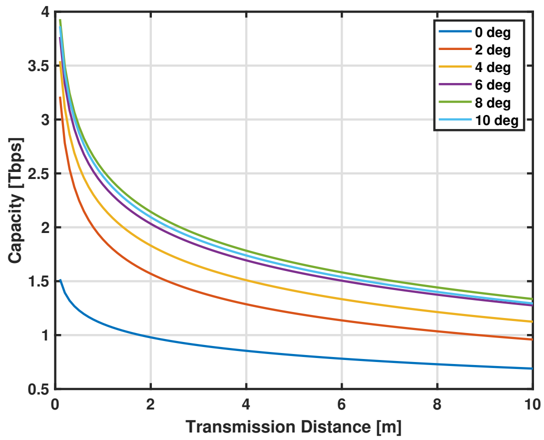

(a) Capacity vs. transmission distance

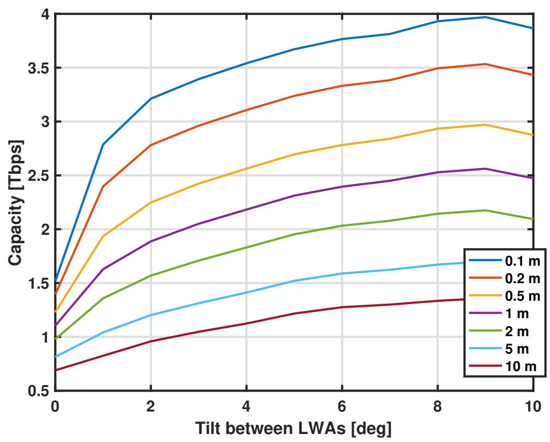

(b) Capacity vs. angle tilt between LWAs

Fig. 5. Capacity in a point-to-point 4×4 MIMO system.

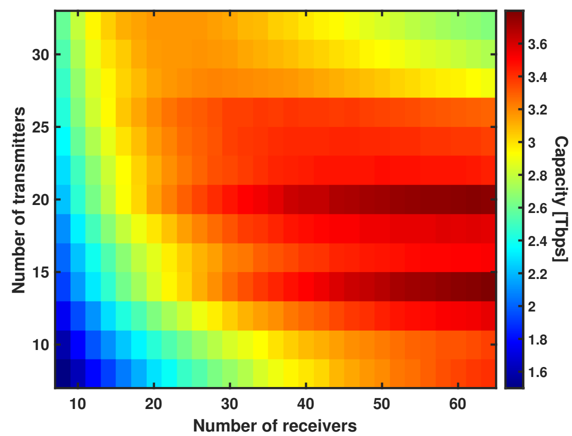

(a) Stair-case LWA array

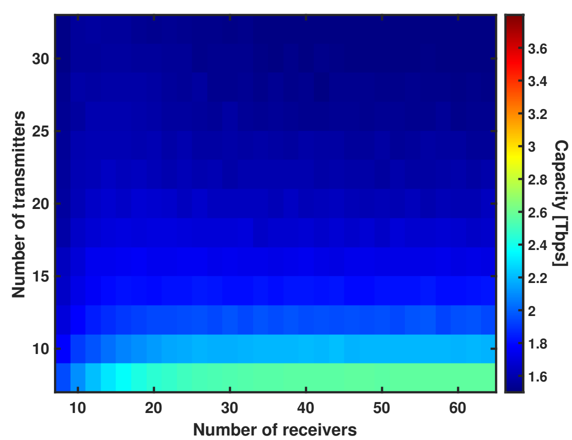

(b) Sectorized antenna array

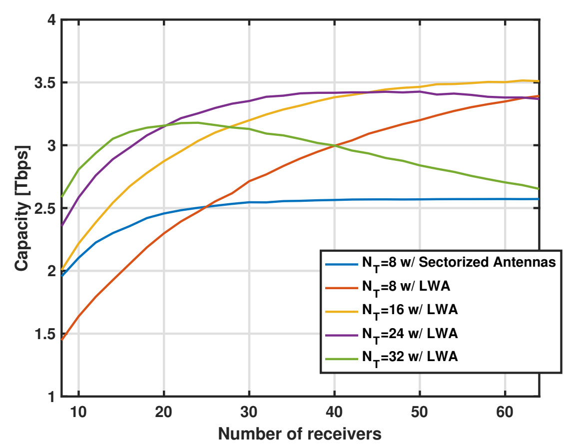

(c) Comparison between both structures

Fig. 6. Capacity in a multi-user MIMO system.

of 10.08 dB, and we will consider this value across the entire bandwidth of interest.

We measured the data rates of the users using (5) for a range of transmit antennas between 8 and 32, and a range of users between 8 and 64. The transmitters were uniformly tilted to cover the 360° range, while the receivers were randomly distributed around a circle at a fixed distance of 10 m from the base station. To obtain average data rates, we generated a large number (1000) of realizations. As in the previous subsection, the total transmit power was set to 1 W, the receiver's temperature was 300 K, and the bandwidth was divided into 1 GHz sub-bands.

Figure 6a and 6b depict the average sum capacities of all users for the stair-case LWA array and the sectorized antenna array, respectively, as a function of the number of transmitters and users in the system. The first plot demonstrates that increasing the number of transmitting LWAs or users leads to a general enhancement in the sum capacities, as discussed in Section III-C. Conversely, the second plot shows that employing 8 transmit antennas for the sectorized antenna array yields satisfactory performance due to its optimal beamwidth of 45°, effectively covering the entire 360° range without causing inter-cell interference. However, increasing the number of transmit antennas becomes counterproductive as it introduces unwanted interference. Moreover, maintaining 8 transmit antennas results in a relatively constant sum capacity even with increasing user numbers, owing to the necessity of each cell within the base station to distribute its bandwidth among its users. A comparison of the sum capacities obtained with both architectures is shown in Fig. 6*c*. Clearly, the former outperforms the latter in most cases. Taking a closer look at the capacities obtained with the stair-case LWA array, it can be observed that raising the number of transmitters has initial benefits, but performance degradation occurs as the number of users surpass a certain threshold. This degradation stems from the fact that with a high number of transmit antennas, their angular separation becomes narrower, leading to interference issues once a certain number of users are present. Hence, the optimal number of transmitters must be chosen based on the specific beamwidth of the LWAs.

V. Conclusions

In this paper, we have proposed the use of LWAs in THz MIMO systems. We have shown that, by introducing a tilt among the elements within a LWA array, we can achieve spatial multiplexing. This technique enables the transmission of independent data streams towards distinct directions, resulting in higher data rates. We support our claims with numerical analyses. Firstly, a tilted LWA array is studied in a point-to-point MIMO channel to showcase how applying a tilt enhances the capacity compared to a uniform LWA array. Secondly, we study a stair-case LWA array in a multi-user MIMO channel and find that it offers substantial advantages over commonly used sectorized antennas in cellular communications. The combination of the high directivity of LWAs and their dynamic beam-steering capabilities provides a pronounced edge in such scenarios, especially in highly dense environments.

References

[1] I. F. Akyildiz, C. Han, Z. Hu, S. Nie, and J. M. Jornet, “Terahertz Band Communication: An Old Problem Revisited and Research Directions for the Next Decade,” *IEEE Transactions on Communications*, vol. 70, no. 6, pp. 4250–4285, Jun. 2022.

[2] J. M. Jornet, E. W. Knightly, and D. M. Mittleman, “Wireless communications sensing and security above 100 ghz,” *Nature Communications*, vol. 14, no. 1, p. 841, 2023.

[3] I. F. Akyildiz and J. M. Jornet, “Realizing Ultra-Massive MIMO (1024×1024) communication in the (0.06–10) Terahertz band,” *Nano Communication Networks*, vol. 8, pp. 46–54, Jun. 2016.

[4] M. Polese, X. Cantos-Roman, A. Singh, M. J. Marcus, T. J. Maccarone, T. Melodia, and J. M. Jornet, “Coexistence and Spectrum Sharing Above 100 GHz,” *Proceedings of the IEEE*, vol. 111, no. 8, pp. 928–954, Aug. 2023.

[5] C. Han, L. Yan, and J. Yuan, “Hybrid Beamforming for Terahertz Wireless Communications: Challenges, Architectures, and Open Problems,” *IEEE Wireless Communications*, vol. 28, no. 4, pp. 198–204, Aug. 2021.

[6] A. Faisal, H. Sarieddeen, H. Dahrouj, T. Y. Al-Naffouri, and M.-S. Alouini, “Ultramassive MIMO Systems at Terahertz Bands: Prospects and Challenges,” *IEEE Vehicular Technology Magazine*, vol. 15, no. 4, pp. 33–42, Dec. 2020.

[7] B. Ning, Z. Tian, W. Mei, Z. Chen, C. Han, S. Li, J. Yuan, and R. Zhang, “Beamforming Technologies for Ultra-Massive MIMO in Terahertz Communications,” *IEEE Open Journal of the Communications Society*, vol. 4, pp. 614–658, 2023.

[8] S. Ju and T. S. Rappaport, “Sub-Terahertz Spatial Statistical MIMO Channel Model for Urban Microcells at 142 GHz,” in *2021 IEEE Global Communications Conference (GLOBECOM)*, Dec. 2021, pp. 1–6.

[9] Y. Xing and T. S. Rappaport, “Propagation Measurements and Path Loss Models for sub-THz in Urban Microcells,” in *ICC 2021 - IEEE International Conference on Communications*, Jun. 2021, pp. 1–6.

[10] H. Do, S. Cho, J. Park, H.-J. Song, N. Lee, and A. Lozano, “Terahertz Line-of-Sight MIMO Communication: Theory and Practical Challenges,” *IEEE Communications Magazine*, vol. 59, no. 3, pp. 104–109, Mar. 2021.

[11] N. Maletic, D. L. Lopacinski, M. Goodarzi, D. M. Eissa, and D. J. Gutiérrez, “A Study of LOS MIMO for Short-Range Sub-THz Wireless Links.”

[12] D. M. Bodet and J. M. Jornet, “Impact of Antenna Element Directivity and Reflection-Interference on Line-of-Sight Multiple Input Multiple Output Terahertz Systems,” in *2022 3rd URSI Atlantic and Asia Pacific Radio Science Meeting (AT-AP-RASC)*, May 2022, pp. 1–4.

[13] C. Lin and G. Y. L. Li, “Terahertz Communications: An Array-of-Subarrays Solution,” *IEEE Communications Magazine*, vol. 54, no. 12, pp. 124–131, Dec. 2016.

[14] H. Zhao, B. Quan, X. Wang, C. Gu, J. Li, and Y. Zhang, “Demonstration of Orbital Angular Momentum Multiplexing and Demultiplexing Based on a Metasurface in the Terahertz Band,” *ACS Photonics*, vol. 5, no. 5, pp. 1726–1732, May 2018.

[15] H. Zhou, X. Su, A. Minoofar, R. Zhang, K. Zou, H. Song, K. Pang, H. Song, N. Hu, Z. Zhao, A. Almaiman, S. Zach, M. Tur, A. F. Molisch, H. Sasaki, D. Lee, and A. E. Willner, “Utilizing multiplexing of structured THz beams carrying orbital-angular-momentum for high-capacity communications,” *Optics Express*, vol. 30, no. 14, p. 25418, Jul. 2022.

[16] D. R. Jackson, C. Caloz, and T. Itoh, “Leaky-Wave Antennas,” *Proceedings of the IEEE*, vol. 100, no. 7, pp. 2194–2206, Jul. 2012.

[17] D. R. Jackson and A. A. Oliner, “Leaky-Wave Antennas,” in *Modern Antenna Handbook*. John Wiley & Sons, Ltd, 2008, pp. 325–367.

[18] H. V. Nguyen, S. Abielmona, A. Rennings, and C. Caloz, “Pencil-Beam Full-Space Scanning 2D CRLH Leaky-Wave Antenna Array,” in *2007 International Symposium on Signals, Systems and Electronics*, Jul. 2007, pp. 139–142.

[19] Y. Geng, J. Wang, Y. Li, Z. Li, M. Chen, and Z. Zhang, “Leaky-Wave Antenna Array With a Power-Recycling Feeding Network for Radiation Efficiency Improvement,” *IEEE Transactions on Antennas and Propagation*, vol. 65, no. 5, pp. 2689–2694, May 2017.

[20] U. Dey, J. Tonn, and J. Hesselbarth, “Millimeter-Wave Dielectric Waveguide-Based Leaky-Wave Antenna Array,” *IEEE Antennas and Wireless Propagation Letters*, vol. 20, no. 3, pp. 361–365, Mar. 2021.

[21] Chien-Jen Wang, Hua-Lin Guan, and C. Jou, “Two-dimensional scanning leaky-wave antenna by utilizing the phased array,” *IEEE Microwave and Wireless Components Letters*, vol. 12, no. 8, pp. 311–313, Aug. 2002.

[22] A. Moldovan, M. A. Ruder, I. F. Akyildiz, and W. H. Gerstacker, “LOS and NLOS channel modeling for terahertz wireless communication with scattered rays,” in *2014 IEEE Globecom Workshops (GC Wkshps)*, Dec. 2014, pp. 388–392.

[23] A. Goldsmith, *Wireless Communications*, ser. Cambridge Core. Cambridge University Press, 2005.

[24] Q. Spencer, C. Peel, A. Swindlehurst, and M. Haardt, “An introduction to the multi-user MIMO downlink,” *IEEE Communications Magazine*, vol. 42, no. 10, pp. 60–67, Oct. 2004.

[25] H. Weingarten, Y. Steinberg, and S. Shamai, “The capacity region of the Gaussian MIMO broadcast channel,” in *International Symposium onInformation Theory, 2004. ISIT 2004. Proceedings.*, Jun. 2004, pp. 174–.

[26] R. C. Johnson, *Antenna Engineering Handbook*. McGraw-Hill, 1993.

[27] N. Javanbakht, B. Syrett, R. E. Amaya, and J. Shaker, “A Review of Reconfigurable Leaky-Wave Antennas,” *IEEE Access*, vol. 9, pp. 94 224–94 238, 2021.

[28] M. Esquius-Morote, J. S. Gomez-Diaz, and J. Perruisseau-Carrier, “Sinusoidally Modulated Graphene Leaky-Wave Antenna for Electronic Beamscanning at THz,” *IEEE Transactions on Terahertz Science and Technology*, vol. 4, no. 1, pp. 116–122, Jan. 2014.

[29] X.-C. Wang, W.-S. Zhao, J. Hu, and W.-Y. Yin, “Reconfigurable Terahertz Leaky-Wave Antenna Using Graphene-Based High-Impedance Surface,” *IEEE Transactions on Nanotechnology*, vol. 14, no. 1, pp. 62–69, Jan. 2015.

[30] N. J. Karl, R. W. McKinney, Y. Monnai, R. Mendis, and D. M. Mittleman, “Frequency-division multiplexing in the terahertz range using a leaky-wave antenna,” *Nature Photonics*, vol. 9, no. 11, pp. 717–720, Nov. 2015.